Alternative generation of well-aligned uniform lying helix texture in a cholesteric liquid crystal cell

Chia-Hua Yu, Po-Chang Wu, and Wei Lee

Citation: AIP Advances **7**, 105107 (2017); doi: 10.1063/1.4995658
View online: http://dx.doi.org/10.1063/1.4995658
View Table of Contents: http://aip.scitation.org/toc/adv/7/10
Published by the American Institute of Physics

Alternative generation of well-aligned uniform lying helix texture in a cholesteric liquid crystal cell

Chia-Hua Yu, Po-Chang Wu, and Wei Lee[a]
College of Photonics, National Chiao Tung University, Guiren, Tainan 71150, Taiwan

(Received 13 July 2017; accepted 3 October 2017; published online 10 October 2017)

This work demonstrates a simple approach for obtaining a well-aligned uniform lying helix (ULH) texture and a tri-bistable feature at ambient temperature in a typical 90°-twisted cell filled with a short-pitch cholesteric liquid crystal. This ULH texture is obtained at room temperature from initially field-induced helix-free homeotropic state by gradually decreasing the applied voltage. Depending on the way and rate of reducing the voltage, three stable states (i.e., Grandjean planar, focal conic, and ULH) are generated and switching between any two of them is realized. Moreover, the electrical operation of the cell in the ULH state enables the tunability in phase retardation via the deformation of the ULH. The observations made in this work may be useful for applications such as tunable phase modulators and energy-efficient photonic devices. https://doi.org/10.1063/1.4995658

I. INTRODUCTION

Short-pitch cholesteric liquid crystal (CLC) with a uniform lying helix (ULH) confined in a typical sandwich cell exhibits unidirectional helical axes aligned in parallel to the substrate plane and behaves as a uniaxial optical plate cut along the optic axis. The ULH as a birefringent structure is attractive due to its unique electro-optical properties attributable to either the flexoelectric or dielectric coupling effect induced by an external voltage, enabling its development for various photonic devices. At low voltages where the dielectric coupling between the CLC molecules and the applied voltage is insufficient to unwind the helix, linear in-plane rotation of the optic axis of ULH can be induced via the flexoelectric effect[1] and the transmittance under crossed polarizers can thus be electrically controlled. Because of the features of sub-millisecond electro-optical response, wide-viewing angle, and linear gray-scale capability, the flexoelectric effect in the ULH texture has widely been considered as a potential mechanism for developing high-speed optoelectronic devices, especially the information displays.[1–5] In contrast, at higher voltages the dielectric effect instead of the flexoelectric one is predominantly manifested. When using LC material with positive dielectric anisotropy, electrical tunability in birefringence of the CLC in the ULH state has been demonstrated by the voltage-induced deformation of the helix through the dielectric effect and its potential applications in phase modulation[6,7] and tunable lasers[8] have been suggested.

It has long been proven difficult to create defect-free ULH alignment with high stability in a simple sandwich cell geometry. To date, various ULH aligning methods involving treatment by external electric field have been propounded. Widely employed in many ULH-related studies, one of the approaches entails the application of a fixed AC voltage across the cell thickness during the isotropic-to-cholesteric phase transition.[9] Together with mechanical shearing,[6] periodic surface anchoring,[10,11] specific rubbing,[12] or polymer stabilization,[13] improved uniformity and stability of the ULH texture have been reported on the basis of this electric-field approach. When fixing the temperature as a constant, ULH alignment can also be generated by a sustaining AC voltage,[14] or

[a]E-mail: wlee@nctu.edu.tw

by gradual increase in applied AC voltage with promoted uniformity by repeatedly adjusting the voltage between higher and lower magnitudes.[15,16] Another electric-field method, enabling the ULH state to be obtained stably via the electrohydrodynamic effect and to electrically switch to the well-known stable Grandjean planar (P) or the focal conic (FC) state, has been proposed for CLCs with large positive dielectric anisotropy and a tristable CLC device is thus introduced.[17] Unfortunately, high-resistivity LC materials adopted in the current display industry are hardly applicable for this electrohydrodynamic-generated ULH texture since a considerable amount of ions is essential to induce the electrohydrodynamic flow.

In this study, we demonstrate a state-of-the-art approach, permitting the generation of a stable and well-aligned ULH texture in a commercial 90°-twisted cell. A CLC material composed of a nematic host with positive dielectric anisotropy is used and the ULH texture is formed when slowly decreasing the voltage to prompt the textural transition from the helix-unwound homeotropic (H) state to the helical CLC state. The electro-optical responses of the cell in the ULH texture induced by the dielectric effect are discussed and the helical-pitch-dependent stability is evaluated. Furthermore, by combining the mechanisms underlying the voltage-induced ULH texture and the alteration between the bistable P and the FC states, we establish a scheme for electrical switching between arbitrarily two of the P, FC, and the ULH states, termed a tri-bistable state switching.

II. EXPERIMENTAL

CLCs with various pitches p were prepared by incorporating proper loadings of a left-handed chiral additive (S5011, HCCH) with a high helical twisting power (HTP ~107 μm^{-1}) into a nematic host (E44, Daily Polymer Co.). The LC E44 selected possesses positive dielectric anisotropy ($\Delta\varepsilon = 17.2$ at the frequency of 1 kHz and temperature of 20 °C) to permit the proposed approach to be effective in the formation of ULH state. In the dilute limit for a small concentration c of S5011 dissolved in E44, the helical pitch length of each prepared CLC is given by $p = 1/(\text{HTP} \times c)$.[18] The CLC with $p = 295$ nm, which is primarily studied in this work, was injected individually into 90°-twisted cells and antiparallel cells. The other CLCs with $p = 160$ nm, 230 nm, and 472 nm were separately injected into 90°-twisted cells for further investigations of the p dependence of the uniformity and stability of the ULH state. Each empty cell was made of two conducting glass substrates covered with polyimide films to promote the desired surface alignment. The alignment layers used in the both types of cells are the same polyimide (Nissan SE-2170), giving a pretilt angle of ~2°. The cell gap is 5.0 ± 0.5 μm for the 90°-twisted cells and 6.5 ± 0.5 μm for the antiparallel cells. All cells have an identical electrode area of 1 cm^2. Note that the cell gap (5.0 ± 0.5 μm) of each 90°-twisted cell was specifically chosen for the demonstration of the cell in the ULH state as a full-wavelength phase plate at the wavelength of 589 nm.

The measurements were performed at ambient temperatures, varying between 24 °C and 26 °C. Square-wave voltages at a fixed frequency of 1 kHz, supplied by an arbitrary function generator (Tektronix AFG-3022B) and an amplifier (TREK Model 603), were applied independently across the cell thickness and the corresponding cholesteric textures were monitored by polarizing optical microscopy (with Olympus BX51) in conjunction with transmission spectroscopy. The spectra were acquired using a high-speed fiber-optic spectrometer (Ocean Optics HR2000+) along with a halogen light source (Ocean Optics HL2000). Furthermore, obtained with an optical analyzer (ELDIM EZContrast 160R), conoscopic images of the cells in the ULH state were utilized to examine the direction of the helical axis. For this measurement, the cell was placed between crossed linear polarizers and the rubbing direction was set parallel to the transmission axis of one of the crossed polarizers. The light source employed is a commercial LC-display-used white light-emitting-diode backlight with an emission spectrum in the visible light regime.

III. RESULTS AND DISCUSSION

Figure 1 schematically illustrates the working principle of the proposed technique for voltage-induced ULH texture with its confirmation by optical images of a 90°-twisted cell and an antiparallel one. This figure presents a steady fall in amplitude of the applied AC (1 kHz) voltage V rather

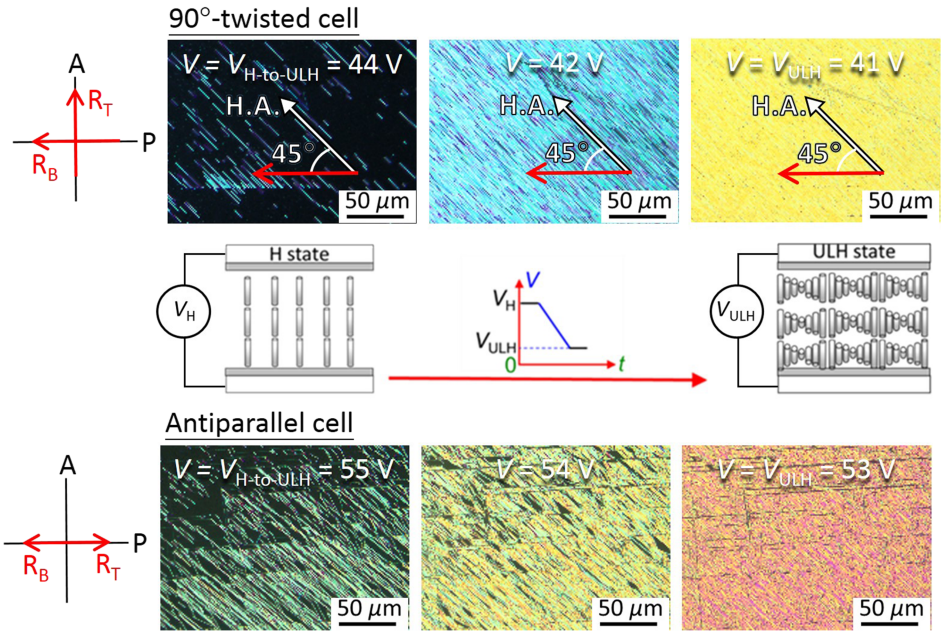

FIG. 1. Voltage-induced textural changes of a 90°-twisted cell and an antiparallel cell (p = 295 nm) in a voltage-descending process from V_H to V_{ULH}, where V_H and V_{ULH} are the 1-kHz voltages for the induction of the homeotropic (H) and the uniform lying helix (ULH) textures, respectively. The analyzer (A) and polarizer (P) are crossed and the rubbing direction of the bottom substrate (R_B) of cells is set parallel to the transmission axis of P. H.A. is the helical axis of ULH stripes.

than the waveform. The voltage-decreasing rate is approximately 0.25 V_{rms}/s. In the case of the 90°-twisted cell, the CLC texture is firstly driven to the H state by voltage $V_H = 45$ V_{rms}. By lowering V slowly from V_H to a critical voltage $V_{H\text{-}to\text{-}ULH}$, a great number of ULH stripes oriented at a specific angle from the rubbing direction start to appear at $V_{H\text{-}to\text{-}ULH}$ = 44 V. These ULH stripes are attributable to the twist deformation of molecules near the surfaces through the helix-unwound homeotropic to the helical CLC transition at this voltage, which is similar to that by the method with a constant voltage applied during the isotropic-to-CLC phase transition.[9] Followed by the expansion and combination of ULH stripes over time during the voltage-decreasing process from $V_{H\text{-}to\text{-}ULH}$ to a holding voltage V_{ULH}, a macroscopically uniform ULH texture eventually appears throughout the entire cell at V_{ULH} = 41 V. Noticeably, the process for the formation of the ULH texture is reversible when increasing V from V_{ULH} through $V_{H\text{-}to\text{-}ULH}$ to V_H. By contrast, while performing the same voltage-descending procedure with the antiparallel cell, the ULH stripes are oriented irregularly at decreasing voltages from $V_H = 56$ V_{rms} to $V_{ULH} = 53$ V_{rms}, resulting in a non-uniform ULH texture. After the removal of the applied voltage, the ULH texture in either the 90°-twisted or antiparallel cell can be preserved with a certain degree of stability depending on the helical pitch length as well as the cell gap (to be discussed later). The effect of the rubbing condition on the ULH structure is further clarified by observing the conoscopic image. One can see from Fig. 2(a) that the ULH texture in the 90°-twisted cell exhibits a unidirectional helical axis with a deviation angle of Ψ with respect to the rubbing direction. In comparison, the antiparallel counterpart displays two helical axes crossed to each other (Fig. 2(b)). Note that the value of Ψ cannot be accurately determined from the conoscopic plots because some experimental errors, arising from the mismatch in position and size of the sample in the optical analyzer (i.e., ELDIM EZContrast 160R), could occur. Nevertheless, the value of Ψ can be preliminarily verified based on the optical textures as depicted in Fig. 1. For the 90°-twisted cell, it is found from Fig. 1(a) that ULH stripes were formed in the direction at an angle of Ψ = 45° with respect to the rubbing direction and this angle remained nearly unchanged when the voltage was decreased from V = $V_{H\text{-}ULH}$ to V = V_{ULH}. Consequently, ideal illustrations of helical axes of ULH alignment based on the abovementioned results can be speculated in considering the effect of cell configuration on the ULH formation. In this study, since the two substrates used are identical, possessing the same anchoring strength and surface polarity, we consider the ULH helical

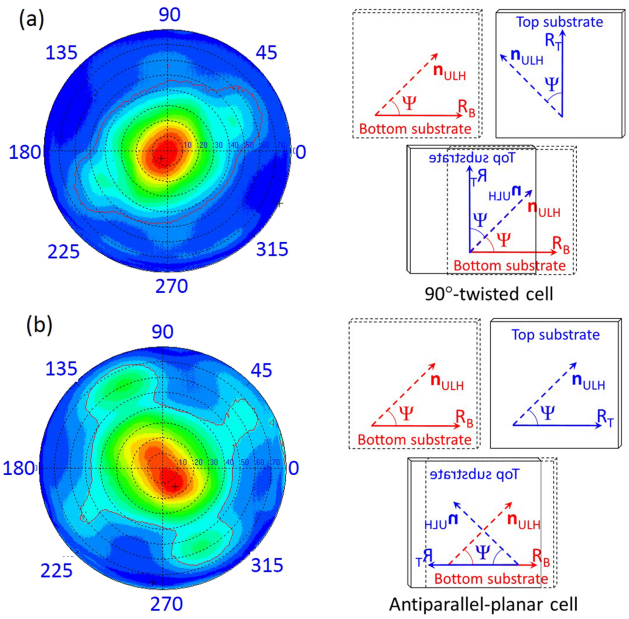

FIG. 2. Conoscopic images and corresponding illustrations of the helical axes of ULH textures in (a) a 90°-twisted cell and (b) an antiparallel cell. p = 295 nm.

axis near each substrate to be counterclockwise deviated at angle Ψ from the rubbing direction. When assembling the top and bottom substrates in a sandwiching manner, the value of Ψ should ideally be 45° so that the ULH alignment could possibly be obtained with a unidirectional helical axis in a 90°-twisted cell (Fig. 2(a)) and with two orthogonal helical axes in an antiparallel cell (Fig. 2(b)). The ideal value of Ψ is consistent with the results given in Fig. 1 and it is actually supported by some of earlier studies. Our approach to the formation of ULH alignment is quite similar to the way with temperature gradient through the isotropic-to-CLC phase transition. It has previously been suggested that a ULH alignment is generated with its helical axis deviating a proper angle Ψ from the rubbing direction. The value of Ψ gets increased with increasing voltage and its maximum depends on the LC material used.[9] In our case, Ψ would be created from a maximum at the vicinity of homeotropic-to-CLC transition in a CLC cell as the voltage is steadily decreased from a higher value (V_H) to the lower one (V_{ULH}). From the point of view of the LC material used, the value of Ψ as large as ~43° using the nematic host E44 has been found in the case of fingerprint helix acquired through the phase transition from the isotropic state to CLC.[19] This supports the ideal value of Ψ ~ 45° in this work as the same LC material E44 is used for preparing the CLC mixture. Moreover, using the LC material E7, Ψ has been suggested to be ~130°; thus, two-domain ULH alignment with nearly orthogonal helical axes in an antiparallel cell has also been found in Ref. 12 by the treatment of voltage applied during the isotropic-to-CLC transition.[12] On the other hand, the orientation of the ULH helical axis could also be reasonably affected by the torques from the top and bottom surfaces. Assume the bulk ULH is undisturbed in the weak-anchoring condition so that the bulk elastic term of free energy is already at minimum. This allows the total free energy in the ULH state to achieve minimum by minimization of the surface contribution. The surface anchoring term of free energy can be expressed by $f_s = (1/2)\ W\ (\sin^2\ \varphi_T + \sin^2\ \varphi_B)$, where W is the azimuthal anchoring energy and φ_T and φ_B are azimuthal angles between the helical axis and the easy axes on the top and bottom substrates, respectively. Let ψ be the angle between the two easy axes ($\psi = \varphi_T - \varphi_B$), then, f_s can be rewritten as $(1/2)\ W\ [\sin^2\ (\varphi_B + \psi) + \sin^2\ (\varphi_B)]$. By taking the first derivative and equating it to zero, one can obtain $\varphi_T = \psi/2$ and $\varphi_B = -\psi/2$. For ULH alignment in the 90°-twisted cell, this means that the helical axis is a bisect of the angle between the easy axes at the substrates. The above interpretations together with the scheme as shown in Fig. 2 are preliminary and the detailed mechanism behind them is considered as a subject for further investigations. Nevertheless, it is ensured, based on the present study, that the uniformity of the ULH texture obtained by the decreasing-voltage

treatment can be improved by optimizing the rubbing directions of the two substrates to impose a sole orientation of ULH axes throughout the cell. While similar results have also been observed in Ref. 12, the ULH alignment is generated by applying a high-magnitude, high-frequency voltage to the cell during the cooling process from the isotropic to the CLC phase and the so-formed ULH structure requires polymer stabilization.[12] In this study, the ULH alignment can be simply obtained at ambient temperature and stably preserved at null voltage by further decreasing the voltage slowly to zero.

To investigate the effect of p on the ULH formation, Fig. 3 shows the transmission spectra and optical textures of four CLC cells in the ULH state. The spectrum of each cell was measured using unpolarized white light but the corresponding optical texture was monitored under crossed polarizers with the rubbing direction of the bottom substrate being parallel to the transmission axis of either linear polarizer. All cells were electrically treated with the proposed voltage-descending method and ULH textures were stably obtained at zero voltage for spectral measurements. While generally defining a texture with a reasonable degree of stability as a stable state, all the four ULH textures are stable and the stability and uniformity degrade over time and decrease with increasing helical pitch. It is found that the ULH can be retained for more than one day in the cell with p = 160 nm and for several hours in the cell with p = 472 nm. Although the spectra of the cells with p = 230 nm and 295 nm are comparable, it is clear from macroscopic inspection that the overall transmission in the ULH state within the visible region decreases as p increases. This can be explained by the increasing amount of defects formed during the voltage-decreasing process from the voltage V_H to zero in the ULH texture with longer pitch, causing stronger scattering to reduce the transmission. Such evidence can be ascertained by the corresponding optical textures in which non-uniform ULH domains, separated by disclinations, are obtained obviously in the cell with p = 472 nm. Moreover, by using the transmittance of the cell in the H state as the reference, the quality of a ULH alignment can be quantified in that the transparency of a perfect ULH alignment should be analogous to that of the H state. In the visible regime of 400–700 nm, all cells in the H state exhibit the same transmission with their transmittance of $T_H \sim 86\%$ and the averaged transmittance of the ULH at $V = 0$ V is $T_{ULH} \sim 74\%$ at p = 160 nm, ~70% at p = 230 nm, ~69% at p = 295 nm, and ~60% at p = 472 nm. The quality of stable ULH alignment is quantitatively indicated by the contrast ratio (CR) of T_{ULH} to T_H (i.e., $CR = T_{ULH}/T_H$). Accordingly, CR is ~0.86 at p = 160 nm, ~0.81 at p = 230 nm, ~0.80% at p = 295 nm, and ~0.70 at p = 472 nm. This suggests that none of the ULH structures with pitch lengths between 160 nm and 472 nm is perfectly uniform. One of the major reasons limiting the quality of ULH alignment is the unexpected surge voltage arising from unavoidable impedance switching between two operation voltage regimes in the voltage-descending process. One can thus expect improved alignment uniformity of ULH by employing a high-precision function generator with an excellent circuital filter to prevent surge voltage. Otherwise, in order to promote the uniformity and stability of the ULH texture in a wider pitch-length range, one can optimize the cell gap or perform polymer stabilization of the ULH texture to create a loose polymer network.[13]

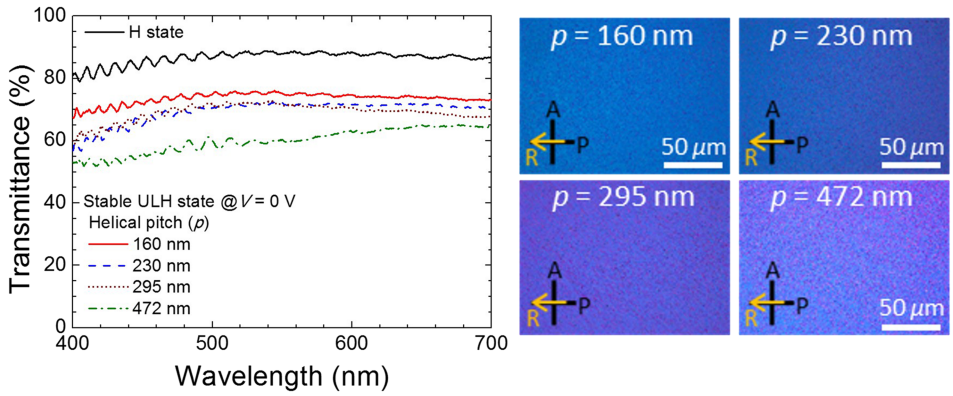

FIG. 3. Transmission spectra of CLC cells by unpolarized light with distinct helical pitches in the ULH state at zero voltage and their corresponding optical textures obtained under crossed polarizers.

The change of ULH orientation in response to the external voltages has been considered superior for modulating the optical properties of the incoming polarized light via either the flexoelectric or dielectric effect. The voltage-dependent intensity of light transmitted through the ULH texture can thus be generally expressed as[20]

$$I = I_0 \sin^2\{2[\Psi_0 + \phi(E)]\} \sin^2\left[\frac{\pi d}{\lambda}\Delta n(E)\right] \quad (1)$$

where I_0 is a constant, Ψ_0 is the angle between the transmission axis of the polarizer and the optic axis of the ULH at zero voltage, λ is the wavelength of the incident light in vacuum. $\phi(E)$ and $\Delta n(E)$ are the in-plane deviation angle of the optic axis and the birefringence of the ULH state, dominated respectively by the voltage-induced flexoelectric and the dielectric switching. Accordingly, while situating the 90°-twisted cell (p = 295 nm) in the ULH state between crossed polarizers at $\Psi_0 = 45°$, the results shown in Fig. 4(a) demonstrate continuous shift of transmission spectra with external voltages, suggesting the ability for modulating the polarization state of light. In this study, because $\Delta\varepsilon$ of the host LC E44 is as large as 17.2, the flexoelectric response to the external field is relatively small and the contribution of $\phi(E)$ to the transmittance of the cell is negligible ($\phi(E) \sim 0$). The intensity of light through the ULH alignment is thus simply a function of $\Delta n(E)$ as Eq. (1) is reduced to $I = I_0 \sin^2[(\pi\, d\, \Delta n(E)) / \lambda]$ at $\Psi_0 = 45°$. While the ordinary and extraordinary refractive indices of the host LC material are respectively denoted as n_e and n_o, the birefringence of a ULH alignment can be expressed as $\Delta n = n_o - n_\perp$. As interpreted in Ref. 20, $n_\perp$ is a function of the voltage-induced deformation of helical profile. The voltage-induced dielectric coupling enables continuous deformation of molecular helix from the uniaxial field-off state, with the optic axis uniformly aligned in the plane of the cell, to the field-on in-plane optically isotropic state (i.e., the H state), giving rise to the change in $n_\perp$ from $(n_e + n_o)/2$ at V = 0 V to n_o at $V = V_H$. This provides the applicability of the proposed ULH alignment as a tunable phase modulator and a designated wave plate. For example, the 90°-twisted cell (p = 295 nm) in the ULH state can be regarded as a full-wavelength plate. In an ideal case for the LC host E44 with n_e = 1.79 and n_o = 1.55 at the wavelength of 589 nm and 20 °C, $\Delta n(E)$ varies from 0.12 to 0 with increasing voltage up to $V = V_H$, and the phase retardation $\delta = (2\pi\Delta nd)/\lambda)$ of the cell with d = 4.9 μm thus experiences a full 2π at λ = 589 nm. Consequently, the transmittance of the cell at this wavelength, as shown in Fig. 4(b), is increased firstly from a minimum (T = 1%) at V = 9 V_{rms} (where $\delta = 2\pi$) to a maximum at V = 40 V_{rms} ($\delta = \pi$) and again decreased to the minimum at V = 45 V_{rms} (δ = 0). The figure reveals a small decrease in transmittance at λ = 589 nm as the voltage grows from 0 V to 9 V_{rms}. Such a small decrease in transmittance is attributable to the tolerance of the cell gap as measured by means of interferometry, making the phase retardation slightly greater than 2π at V = 0 V.

The alluring nature of the proposed ULH state includes not only its optical stability but the electrical switchability to other stable states (i.e., P and FC states). It is illustrated in Fig. 5 that switching between arbitrarily two states can readily be realized by applying a voltage (V_H) to firstly

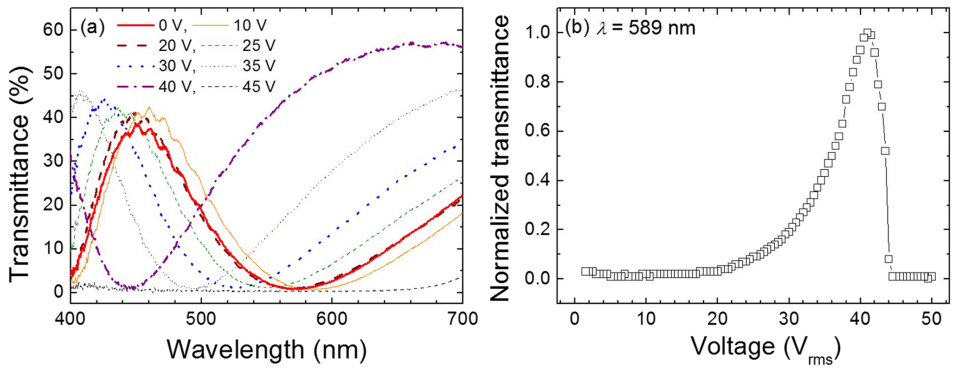

FIG. 4. (a) Transmission spectra of the 90°-twisted cell (p = 295 nm) in the ULH state at various AC voltages, and (b) voltage dependence of the transmission of the cell at wavelength of 589 nm (data retrieved from (a)). The cell is placed between crossed linear polarizers.

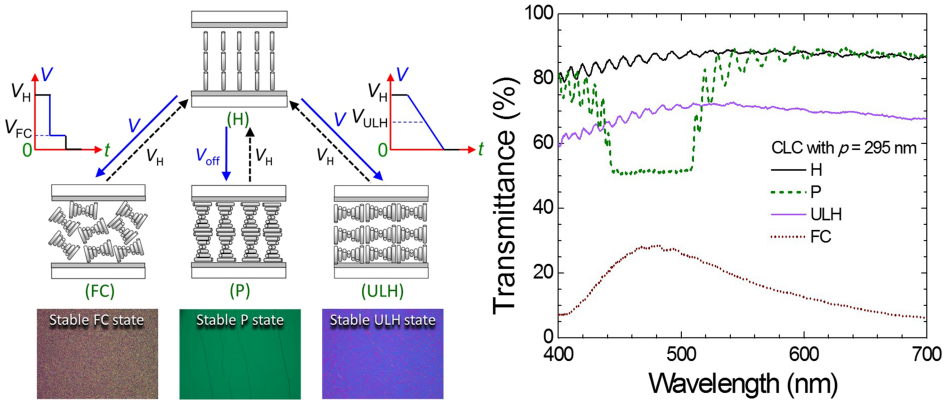

FIG. 5. Schematic of the tri-bistable switching among the P, the FC and the ULH states with corresponding textural and spectral confirmations in a CLC cell with 90°-twisted surface alignment.

sustain the cell to the H state, followed by the control of the voltage-decreasing rate. This operation scheme for tri-bistable switching among P, FC, and ULH states is quite different from that suggested in Ref. 17 where CLC material with considerably high ion concentration is required to switch the CLC from either state to the ULH state by a low-frequency voltage via the electrohydrodynamic effect. In our case, the voltage-induced electrohydrodynamic effect can be ruled out because the frequency is 1 kHz, which is much higher than the relaxation frequency of space-charge polarization. Moreover, due to the use of the LC material (E44) with relatively high dielectric anisotropy, the flexoelectric response of the ULH alignment to the voltage is suppressed and textural switching as depicted in Fig. 5 is presumably attributed to the dielectric coupling. For instance, turning off the voltage rapidly from V_H results in the relaxation of the molecular helix back to the stable P state. The P state can be regarded as the color-reflective state whose reflection band is designable by controlling the content of the chiral additive in the nematic host. When switching the voltage directly from V_H to V_{FC} and then turning off the voltage, the cell becomes stable in the FC state, serving as a light-opaque state owing to the randomly oriented molecular helix to scatter light. Note that V_{FC} is a voltage higher than the onset voltage for P-to-FC transition. In Fig. 5, optical texture and transmission spectrum of the stable FC state were obtained by switching the voltage directly from V_H = 45 V_{rms} to V_{FC} = 30 V_{rms} and then to V = 0 V. More importantly, when decreasing the voltage from V_H gradually through V_{ULH} to zero at the same rate, a stable ULH state can be attained. The ULH state capably serves as the light-transmission state due to the uniaxial optical feature. As exemplarily evidenced by optical images and spectral properties of the CLC cell with p = 295 nm in the three stable states (Fig. 5), the cell can be used as a light shutter in transmissive mode by the FC–ULH switching and reflective mode by the FC–P or ULH–P switching. As such, the proposed driving scheme for tri-bistable state switching is simple, compatible of use to currently available CLC-based light shutters with promoted flexibility.

IV. CONCLUSIONS

In conclusion, we have demonstrated an approach to the formation of stable ULH alignment in a CLC cell at ambient temperatures. By first applying a sufficiently high voltage to induce the H state, subsequent slow decrease in voltage, say, with a rate of −0.25 V_{rms}/s, has been proven effective to obtain well-aligned ULH texture in a 90°-twisted cell. Such a ULH texture has been explained by the induction of the structural transition from the homeotropic nematic to the helical CLC alignment and thus the twist deformation near the substrate surfaces during the voltage-decreasing process. Compared with other ULH generation methods, our proposed one is applicable to most of positive LC material and it is simple because none of temperature gradient, mechanical shear, or electrohydrodynamic flow is required. It is ensured that the well-aligned ULH can be readily reproduced via our proposed approach. Parameters such as the cell gap, pretilt angle, and surface anchoring strength that can affect the alignment uniformity of ULH state will be further investigated

towards the development of best solution of high-quality ULH alignment. The ULH state resembling a uniaxial crystal allows electrical tunability in phase retardation. Moreover, an innovated scheme, enabling the tri-bistable switching among P, FC and ULH, is established by combining our proposed approach with the general scheme for bistable switching between the P and the FC states. As a result, the proposed approach is beneficial for CLC to be designed as phase modulators and energy-efficient light shutters.

ACKNOWLEDGMENTS

The authors gratefully acknowledge Lachezar Komitov for helpful discussion and constructive comments. This study was financially supported by the Ministry of Science and Technology, Taiwan, under Grant Nos. 104-2112-M-009-008-MY3 and 106-2923-M-009-002-MY3.

[1] J. S. Patel and R. B. Meyer, Phys. Rev. Lett. **58**, 1538 (1987).
[2] D. J. Gardiner, S. M. Morris, P. J. W. Hands, F. Castles, M. M. Qasim, W.-S. Kim, S. S. Choi, T. D. Wilkinson, and H. J. Coles, Appl. Phys. Lett. **100**, 063501 (2012).
[3] B. I. Outram and S. J. Elston, J. Appl. Phys. **113**, 043103 (2013).
[4] Y. Inoue and H. Moritake, Appl. Phys. Express **8**, 071701 (2015).
[5] Y. Inoue and H. Moritake, Appl. Phys. Express **8**, 061701 (2015).
[6] P. Rudquist, L. Komitov, and S. T. Lagerwall, Liq. Cryst. **24**, 329 (1998).
[7] R. M. Hyman, A. Lorenz, and T. D. Wilkinson, Liq. Cryst. **43**, 1 (2016).
[8] H. Yoshida, Y. Inoue, T. Isomura, Y. Matsuhisa, A. Fujii, and M. Ozaki, Appl. Phys. Lett. **94**, 093306 (2009).
[9] S. D. Lee and J. S. Patel, Phys. Rev. A **42**, 997 (1990).
[10] L. Komitov, G. P. B. Brown, E. L. Wood, and A. B. J. Smout, J. Appl. Phys. **86**, 3508 (1999).
[11] G. Hegde and L. Komitov, Appl. Phys. Lett. **96**, 113503-1–113503-3 (2010).
[12] P. S. Salter, S. J. Elston, P. Raynes, and L. A. Parry-Jones, Jap. J. Appl. Phys. **49**, 101302 (2009).
[13] S. H. Kim, L.-C. Chien, and L. Komitov, Appl. Phys. Lett. **96**, 161118 (2005).
[14] D. Subacius, P. J. Bos, and O. D. Lavrentovich, Appl. Phys. Lett. **71**, 1350 (1997).
[15] A. Varanytsia and L.-C. Chien, J. Appl. Phys. **119**, 014502 (2016).
[16] A. Varanytsia and L.-C. Chien, Sci. Rep. **7**, 41333 (2017).
[17] C.-T. Wang, W.-Y. Wang, and T.-H. Lin, Appl. Phys. Lett. **99**, 041108 (2011).
[18] R. Cano and P. Chatelain, C. R. Acad. Sci., Paris **B259**, 252 (1964).
[19] R. S. Zola, L. R. Envangelista, Y.-C. Yang, and D.-K. Yang, Phys. Rev. Lett. **110**, 057801 (2013).
[20] P. Rudquist, L. Komitov, and S. T. Lagerwall, Phys. Rev. E **50**, 4735 (1994).